Journal of Statistical Physics, Vol. 91, Nos. 1/2, 1998

Cluster Structure of Collapsing Polymers

R. Brak,[1] P. P. Nidras,[1] and A. L. Owczarek[1]

Received August 22, 1997; final January 28, 1998

In order to better understand the geometry of the polymer collapse transition, we study the distribution of geometric clusters made up of the nearest neighbor interactions of an interacting self-avoiding walk. We argue for this new correlated percolation problem that in two dimensions, and possibly also in three dimensions, a percolation transition takes place at a temperature *lower* than the collapse transition. Hence this novel transition should be governed by exponents unrelated to the θ-point exponents. This also implies that there is a temperature range in which the polymer has collapsed, but has no long-range cluster structure. We use Monte Carlo to study the distribution of clusters on the simple cubic and Manhattan lattices. On the Manhattan lattice, where the data are most convincing, we find that the percolation transition occurs at $\omega_p = 1.461(3)$, while the collapse transition is known to occur exactly at $\omega_\theta = 1.414...$. We propose a finite-size scaling form for the cluster distribution and estimate several of the critical exponents. Regardless of the value of ω_p, this percolation problem sheds new light on polymer collapse.

KEY WORDS: Droplets; percolation; self-avoiding walks; polymer collapse.

1. INTRODUCTION

The collapse transition of long chain polymers in dilute solution is one of the most studied phase transitions in statistical mechanics.[1, 2, 3] This transition is characterised by the sharp change in large-molecular-weight scaling properties of a single polymer on lowering the temperature. At fixed, high temperatures the large molecular weight limit of polymers in dilute solution has been understood to be a critical phenomenon in its own right:[4] there is a correspondence to the O(n) spin model in the limit $n \to 0$. This phenomenon itself involves the so-called excluded volume problem which

[1] Department of Mathematics, University of Melbourne, Parkville, Victoria 3052, Australia; e-mail: {brak, ppn, aleks}@maths.mu.oz.au.

0022-4715/98/0400-0075$15.00/0

implies that in low dimensions polymers will take up much more volume than one would expect from a naive random walk model. The addition of attractive interactions complicates the situation and allows for a crossover to a state which is more compact than a random walk and in fact is dense in space on lowering the temperature (increasing the strength of the attraction). This collapse transition (which occurs at the θ-point) for a single polymer from an expanded to an internally-dense state has been conjectured to be described by a tricritical O(n) field theory.[2, 5]

To facilitate physical understanding of the renormalisation group approach to the polymer collapse transition de Gennes[2, 5] introduced the associated "blob" picture of the approach to the collapse point. In contrast to this elegant but essentially mathematical picture we are interested in the question of whether, on lowering the temperature through the collapse temperature, some sort of percolation transition takes place as a result of the inevitable *clustering* of the polymer. It would seem natural to assume that it does since at very low temperatures the polymer is almost completely compact and so large multiply-connected clusters should exist, while at high temperatures the polymer forms a random fractal. One way to view the collapse process might then be through the clustering of the polymer to form dense regions. This clustering should admit the possibility of a percolation phenomenon. In this paper we study this question of percolation associated with polymer collapse in some depth by considering the *percolation of interactions*. We do this because the geometry of the interactions gives us new information on the structure of the polymer conformation. Of course, there may be other percolation processes of interest in conjuction with polymer collapse.

One avenue of study of the collapse transition has been to model the geometry of a polymer by a self-avoiding walk (SAW) on a regular lattice, which incorporates directly the excluded volume, and the interactions between monomers by nearest-neighbour contact potentials. This model of a polymer in solution shall form the basis of our studies here. To define a percolation problem one must define at least two things: First, one must define what it is that might be percolating and second one must specify the connectedness rule.

The self-avoiding walk model in conjuction with the motivation stated above, leads us to focus on the nearest-neighbour interactions of the interacting self-avoiding walk model (ISAW) and the monomers (sites) to which they are connected. Specifically, it is the clustering and percolation properties of the nearest-neighbour interactions themselves that we study. Given that we are focusing on the percolation properties of nearest-neighbour contacts of ISAWs there is still scope to study a variety of percolation models within this context. All these different models are defined

by the choice of connectedness rule. We have chosen one particular simple local rule explained below.

We could of course have chosen different models to explore the question of the percolation of interactions in polymer collapse. As explained above we could have chosen a more general interacting SAW model which includes next nearest-neighbour interactions (or some other such extension). We may also have chosen a different connectedness rule. (One needs to be a little careful in deciding on the exact percolation clustering rule since the walk (polymer) is itself a connected object (if considered by its monomers alone).) We suspect that given that these changes are local and short-ranged that any universal properties of the critical phenomena we discover should be invariant, as these changes do not affect the universality class in other percolation problems. This remains to be verified by future studies. There are arguments for and against different rules but the large computational resources required by the investigation restricted us to investigating only one rule. We therefore chose what we considered the simplest non-trivial rule.

For the reasons given above we have examined the case of bond percolation where the bonds over which the interactions act become the bonds of the percolation process.[2] Two interaction bonds are considered adjacent if they have ends that are no more than one step of the walk apart: this implies they are either directly connected or a step of the walk intervenes. A cluster is a set of adjacent interaction bonds, see Fig. 1. Our cluster number statistics, n_s, count the (weighted) average number of clusters per step for the number of bond interactions, s. This simple definition implies that the average energy U of N-step walks is simply related to the values of n_s by

$$U = -\varepsilon \sum_{s=1}^{s_{\max}} s n_s \tag{1}$$

where $-\varepsilon$ is the energy of a single nearest-neighbour interaction and the maximum size cluster, $s_{\max}$, is proportional to N.

To briefly summarise our work, we find that a percolation transition does indeed take place but at a temperature below the θ-point in two dimensions. The same scenario probably holds in three dimensions but our evidence is less conclusive there. We provide estimates for the associated exponents at this novel transition—which we label "Polymer-Interaction

[2] Please note that we are *not* considering random-interaction models of interacting polymers: in each realisation of our polymer all the interactions that exist are counted as they are, and we do not choose the bonds of the percolation problem directly with an uncorrelated random process.

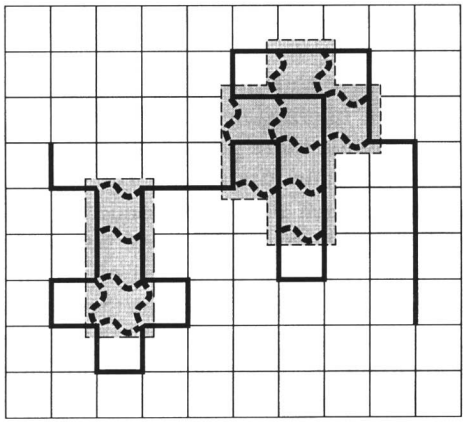

Fig. 1. An interacting self-avoiding walk on the square lattice with two clusters highlighted by shading. The walk is the heavy solid line. The interactions are marked as wavy dashed lines. One cluster is of size 6 and the other is of size 10.

Percolation" (PIP). One may contrast this with the situation of the Ising model in two dimensions[6] where the thermal and percolative transitions take place at the same temperature. Our results imply that there is a range of temperatures for which a polymer is in a collapsed state but contrastingly the interactions do not percolate. In other words there is a macroscopic density (with respect to the underlying lattice, see Eq. (4)) of bonds but no macroscopic structure. We note that the PIP transition is unrelated to the first-order liquid-solid transition of Zhou *et al.*[7] We also note that by analogy to percolation associated with Ising models that the our PIP should not *necessarily* give rise to a singularity in any thermodynamic functions, such as the free energy. Therefore, if the PIP transition does indeed take place away from the θ-point we do not expect any singularity in the free energy, and we have not encountered any evidence to the contrary.

We have explored the questions raised in the model explained above by utilising various contemporary Monte Carlo methods. Our most convincing results come from simulations on the Manhattan lattice where the exact collapse transition temperature (as defined by the change in the exponent ν) is known.[8,9] (We point out that subsequently, the specific heat was shown to be singular at this point.[10]) Simulations there (using kinetic growth algorithms, for example see ref. 10) show fairly conclusively that the expected cluster size is finite (less than 3000 bonds) at the collapse transition temperature. These simulations are for walks of length 10^5 and thus finite size effects are expected to be insignificant.[10] This result implies that,

irrespective of the estimate, given below, of ω_p, the clusters do not percolate at $\omega = \sqrt{2}$.

Using a reptation-based algorithm[11] the PIP transition point has been estimated to be at $\omega = \exp(\varepsilon/k_B T) = 1.461(3)$, where the estimates are systematically moving *away* from the exact collapse point at $\omega = \sqrt{2}$. The fundamental percolation exponents σ and τ have been estimated on this lattice as 0.45(10) and 2.25(15) respectively (c.f. ordinary uncorrelated percolation where $\sigma = 0.3956...$ and $\tau = 2.0549...$). As the walks involved in these estimates are not as long as those involved in the kinetic growth simulations, finite size corrections may still be significant and hence these estimates may be biased.

The possibility that the oriented nature of the Manhattan lattice affects the universality of these exponents and hence the coincidence of the PIP and θ points, are issues we do not address in this paper. However, we point out that the oriented nature of this lattice does not seem to affect the collapse crossover exponent.[10]

We have also carried out simulations on the cubic lattice. Here the collapse and percolation points seem to be distinct though close. We have estimated the exponents at the percolation point on this lattice: the results are given in Section 4.1.

However, we realize that on both lattices, particularly the simple cubic, our estimates for the PIP transition points and the associated best current estimates of the θ points are close. Taking a pessimistic view of corrections to scaling and possible metastability of our simulations, might lead one to believe that the PIP transition in fact takes place at the θ-point. If this were indeed the case one might consider it an even more interesting description of collapse. We believe that the resolution of this question will take substantial computer resources.

In the next section we develop the scaling theory we believe applies to collapsing polymers and our PIP. Following that we detail the Monte Carlo and kinetic walk algorithms that have been used for the simulations. The results are presented and discussed in Section 4.

2. THE PIP TRANSITION AND CLUSTER SCALING

A SAW is a non-intersecting path of $N+1$ contiguous occupied sites of some graph. (In this paper we will be dealing exclusively with regular lattices.) In the ISAW model each non-consecutive nearest-neighbour pair of sites on the walk is assigned a Boltzmann weight ω, with the partition function of walks of length N given as

$$Z_N(\omega) = \sum_{\varphi_N \in \Omega_N} \omega^{m(\varphi_N)} \tag{2}$$

where Ω_N is the set of all N-step SAW and $m(\varphi_N)$ is the number of interactions in the configuration φ_N. The behaviour of this model is characterised by three regimes. There exists a value of $\omega = \omega_\theta$ known as the collapse or θ-point such that the scaling of important quantities is different if ω is fixed below, at or above this value. For $\omega < \omega_\theta$ the radius of gyration scales as $R_G(N) \sim N^{\nu_+}$, where $\nu_+ = 3/4$ in two dimensions and $\nu_+ \approx 0.588$ in three dimensions. For $\omega > \omega_\theta$ the walk is in a dense collapsed state where $R_G(N) \sim N^{1/d}$, d being the dimension. Close to ω_θ there is a tricritical crossover region. Furthermore scaling of R_G at ω_θ gives behaviour intermediate between the two regimes with $R_G(N) \sim N^{\nu_t}$ and $1/d \leqslant \nu_t \leqslant \nu_+$.

On the other hand, the clustering behaviour of the percolation problem we have defined associated with the ISAW model can be understood through the behaviour of the mean number of clusters per monomer of size s, $n_s(\omega, N)$. A plot of n_s for the simple cubic lattice at $\omega = 1.405$ is given in Fig. 2. This function enables the determination of the PIP critical point by the location of the singularities in its thermodynamic limit, $n_s(\omega, \infty) = \lim_{N \to \infty} n_s(\omega, N)$. The mean numbers of clusters per monomer of size s, $n_s(\omega, N)$, or "cluster numbers" are defined as

$$n_s(\omega, N) = \frac{1}{NZ_N(\omega)} \sum_{\varphi_N \in \Omega_N} (\text{Number of clusters of size } s \text{ in walk } \varphi_N)\, \omega^{m(\varphi_N)} \tag{3}$$

where $Z_N(\omega)$ is the partition function of walks of length N as defined above. Note that by dividing by N the cluster numbers $n_s(\omega, \infty)$ are non-zero for

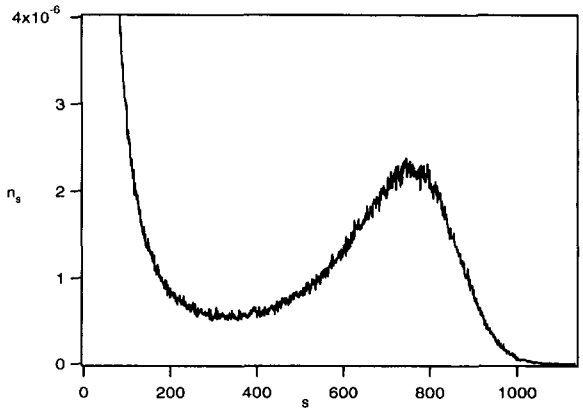

Fig. 2. A plot of the cluster numbers, n_s, vs. the cluster size, s for the simple cubic lattice at $\omega = 1.405 > \omega_p$. This function does not simply decay with increasing s because this data was taken from the low-temperature percolated phase where there is a precursor of the infinite cluster in finite samples.

all finite ω. If one had chosen to divide by the volume of the walk R_G^d then $n_s(\omega, \infty)$ would be non-zero only when the density of the walk is non-zero.

We define the PIP transition point as the temperature at which the higher moments of $n_s(\omega, \infty)$ diverge: this is one of several equivalent ways to define any percolation transition, see Stauffer and Aharony.[12] It would be interesting to base a study of this same problem using a suitable definition of a spanning cluster. We would, of course, expect the conclusions to be exactly the same.

2.1. Density of Interaction Bonds

To understand where a possible PIP transition point, ω_p, might occur we must first consider the interaction bond density ρ of the ISAW model. This is because we assume that for percolation to occur one must have an effective density ρ greater than some transition value ρ_c.

The box density of interaction bonds, $\rho_N(\omega, L)$ is defined as follows: For any given ISAW, φ_N, place a d-dimensional hypercube (or box), B_{L^d}, at the centre of mass of the N-step walk, then

$$\rho_N(\omega, L) = \frac{1}{L^d Z_N(\omega)} \sum_{\varphi_N \in \Omega_N} m(\varphi_N, B_{L^d})\, \omega^{m(\varphi_N)} \tag{4}$$

where $m(\varphi_N, B_{L^d})$ is the number of interaction bonds in the box B_{L^d} for walk φ_N. Then the density is defined as

$$\rho(\omega) = \lim_{L \to \infty} \lim_{N \to \infty} \rho_N(\omega, L) \tag{5}$$

The expected behaviour of the density of interaction bonds is shown schematically in Fig. 3. For $L \ll R_G$ the box density of interaction bonds is generically expected to scale as $L^{1/\nu - d}$, since the total number of interaction bonds at fixed ω inside a box of size L^d, is asymptotically proportional to $L^{1/\nu}$. Since ν is believed to be greater than $1/d$ in the expanded phase we have that $\rho(\omega < \omega_\theta) = 0$. In the collapsed phase $\nu = 1/d$ and hence the density can be non-zero. At the critical point the behaviour depends on the value of ν_t, if $\nu_t > 1/d$, then the density is expected to go continuously to zero as illustrated in Fig. 3. If $\nu_t = 1/d$ then the density will be discontinuous.

If we assume that $\nu_t > 1/d$ as numerical evidence has suggested in two and three dimensions then the PIP transition point obeys $\omega_p > \omega_\theta$ since one expects that it is necessary for $\rho_c = \rho(\omega_p) > 0$ for a short range percolation

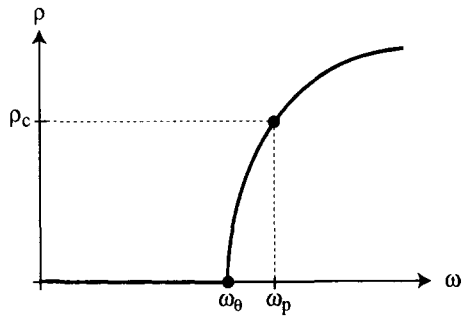

Fig. 3. A schematic illustration of the expected behaviour of the interaction bond density $\rho(\omega)$ as a function of the Boltzmann weight ω.

problem. Hence there are two caveats: if either $\nu_t = 1/d$ or the correlated percolation problem we have defined percolates for *any* concentration (that is, $\rho_c = 0$) then the scenario we paint below needs modification.

This leads us to expect that $\omega_p > \omega_\theta$, with usual percolation-type scaling forms holding around ω_θ and exponents unrelated to those for the thermal collapse around ω_θ. We expand on this below.

2.2. Cluster Scaling

Given that the assumptions discussed above are valid we now explain the crossover and finite-size scaling we expect to occur close to the PIP transition.

The cluster numbers are expected to have a generic percolation type critical point, at ω_p, with associated scaling as well as finite size scaling (i.e., N dependence). Thus, in the limiting region $s \to \infty$, $N \to \infty$ and $\omega \to \omega_p$ we assume that $n_s(\omega, N)$ is a generalized homogeneous function which, in the usual way, leads to the following three equivalent scaling forms

$$n_s(\omega, N) \backsim s^{-\tau} \mathscr{F}_1(s\, \Delta\omega_p^{1/\sigma}, sN^{-\phi_p/\sigma}) \tag{6}$$

$$n_s(\omega, N) \backsim N^{-\tau\phi_p/\sigma} \mathscr{F}_2(\Delta\omega_p N^{\phi_p}, sN^{-\phi_p/\sigma}) \tag{7}$$

$$n_s(\omega, N) \backsim \Delta\omega_p^{\tau/\sigma} \mathscr{F}_3(s\, \Delta\omega_p^{1/\sigma}, \Delta\omega_p N^{\phi_p}) \tag{8}$$

where $\Delta\omega_p = \omega - \omega_p$. For a definition of the "scales as" symbol, $\backsim$, see Brak and Owczarek.[13, 14]

In the analysis of our simulations we will use the scaling of the moments of the cluster numbers to obtain estimates of the critical exponents. The moments are defined as

$$M_k(\omega, N) = \sum_{s=1}^{s_{\max}-1} s^k n_s \tag{9}$$

The summation does not include $s_{\max}$ so as to exclude any infinite cluster that may exist in the thermodynamic limit. Using (8) and approximating the sum by an integral gives

$$M_k(\omega, N) \backsim \Delta\omega_p^{(\tau-k-1)/\sigma} \mathscr{H}'_k(N\,\Delta\omega_p^{1/\sigma}, N^{\phi_p}\,\Delta\omega_p) \tag{10}$$

If we now make a second major assumption that in the limiting region, $N \to \infty$ and $\omega \to \omega_p$, the moment $M_k(\omega, N)$ is a generalized homogeneous function, then this assumption is only consistent with (10) if the two variables $z_1 = N\,\Delta\omega_p^{1/\sigma}$ and $z_2 = N\,\Delta\omega_p^{1/\phi_p}$ are identical, which is the case if $\phi_p = \sigma$. Thus with this assumption we have that

$$M_k(\omega, N) \backsim \Delta\omega_p^{(\tau-k-1)/\phi_p} \mathscr{H}_k(N^{\phi_p}\,\Delta\omega_p) \tag{11}$$

with

$$\mathscr{H}_k(x) \sim \begin{cases} \text{constant} & x \to \infty \\ x^{-(\tau-k-1)/\phi_p} & x \to 0 \end{cases} \tag{12}$$

The asymptotic behaviour of the scaling function $\mathscr{H}_k(x)$ is determined by the fact that $M_k(\omega, N)$ is finite as $N \to \infty$ for $\omega \neq \omega_p$ and that $M_k(\omega_p, N)$ must be independent of ω.

From (11) we deduce that

$$M_k(\omega_p, N) \sim N^{(k+1-\tau)} \qquad \text{as} \quad N \to \infty. \tag{13}$$

Furthermore, as the moments have a maximum, it follows from (12) that the position of this maximum, ω_{Max}, should approach the critical temperature, ω_p, like

$$\omega_p - \omega_{\text{Max}} \sim N^{-\phi_p} \qquad \text{as} \quad N \to \infty \tag{14}$$

Thus, using numerical data in conjunction with (13) and (14), we can get independent estimates of ω_p, τ and ϕ_p.

Analogous to conventional percolation we expect that in the low density phase, $\rho < \rho_c$, that is $\omega < \omega_p$, the cluster numbers in the thermodynamic limit at fixed ω should behave like

$$n_s(\omega < \omega_p, N = \infty) \sim s^{-\tau_-} \exp(-s/s_\xi) \qquad \text{as} \quad s \to \infty \tag{15}$$

where the "typical" cluster size is expected to behave like $s_\xi \sim A\omega_p^{-1/\phi_p}$, and τ_- is another exponent, appearing in the low density regime only. For an infinite length walk there is, of course, no N dependence, and the scaling behaviour is directly analogous to standard percolation. Hence there will be a corresponding set of scaling relations between all the percolation type exponents as there is in standard percolation. We point out that while the moments of the cluster numbers (and $s_\xi(\omega)$) are finite at ω_θ and surely continuous as a function ω below ω_p there should still exist a weak singularity in the cluster numbers (and more precisely $s_\xi(\omega)$) at ω_θ. This is simply because $\rho(\omega)$ is a non-analytic function of ω at ω_θ. Note $\rho = 0$ for $\omega < \omega_\theta$ does *not* imply that $s_\xi = 0$.

3. THE ALGORITHMS

Three different algorithms were employed in the simulations that we conducted. Firstly, we needed an algorithm to simulate ISAWs on the simple cubic and Manhattan lattices for varying ω. We chose to use the enhanced reptation-Metropolis (R-M) algorithm[11] for this purpose. This algorithm had to be slightly modified for the simulations on the Manhattan lattice. The modification made in this case was the omission of the kink-end and end-kink moves since they are not possible for walks on the Manhattan lattice. This however, does not affect the ergodicity (and hence the validity) of the enhanced R-M algorithm because there are no self-trapping ISAW configurations on the Manhattan lattice. We also used a simple static Monte Carlo algorithm to simulate kinetic growth walks (KGWs) on the Manhattan lattice; details of the algorithm can, for example, be found in ref. 10. The two algorithms mentioned above were used to generate the relevant walks with the correct probability distribution. However, we also needed to develop an algorithm to collect the statistics on the cluster numbers for a particular walk. This algorithm was based on the Hoshen–Kopelman algorithm[15] which is used to collect statistics of percolation clusters in a box. We now briefly illustrate how our algorithm works; we will be using the ISAW configuration in Fig. 4 as an example.

Our cluster counting algorithm works by assigning a *non-negative* label to each site of the walk. Each cluster is assigned its own positive label so that interaction bonds whose ends (i.e., the sites of the walk) have the

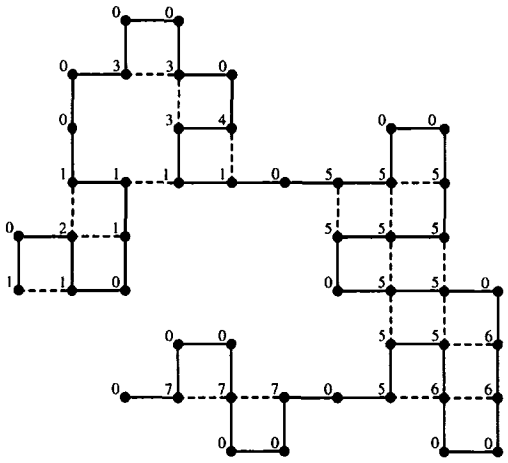

Fig. 4. An example of an ISAW configuration which has been labelled with our cluster labelling algorithm.

same label are part of the same cluster. The algorithm begins by initialising the labels on all the sites of the walk to 0. The algorithm then visits each site of the walk in succession, beginning at one of the endpoints (in the case of Fig. 4, the left-hand end labelled 1). At each site, a check is made for (non-consecutive) nearest neighbour sites. If none are detected, then the site is labelled with a 0; otherwise, the site is assigned a positive label. The value of this label is chosen to be the smallest positive label of its neighbouring sites—including the site immediately preceding the current site. Thus there are three possibilities: (i) all of the neighbouring labels are 0; (ii) all of the positive neighbouring labels are the same; and (iii) some of the positive neighbouring labels differ. If case (i) occurs, then a new label is assigned to the site. In Fig. 4, this occurs with the site labelled 2 since the preceding site is labelled 0, and the two nearest neighbour sites were as yet unvisited and also labelled 0. In case (ii), there is no conflict between the labels so that the new site assumes the label of the other positive labels. In case (iii) the label of the new site is chosen to be the smallest of the positive neighbouring labels. However, there is a conflict between the other labels (i.e., the corresponding sites are part of the same cluster but have different labels) which has to be resolved. To do this, we need an array of labels which will allow us to check the "status" of any given label. A label can be in one of two states: *valid*, or *invalid*. So for case (iii), let the value of the smallest positive neighbouring label be l. Then for each positive neighbouring label different to l, we change its entry in the array of labels to $-l$, where the negative sign indicates that this label is invalid and hence redundant.

Table 1. Example of Evolution of the Label List Used in the Droplet Cluster Labeling Algorithm[a] as Applied to the Example Walk in Fig. 4[b]

Label List \ Time Step	1	3	4	11	16	17	18	21	33	38	42
1	1	1	1	1	1	1	1	1	1	1	1
2		2	−1	−1	−1	−1	−1	−1	−1	−1	−1
3				3	3	3	−1	−1	−1	−1	−1
4					4	−3	−3	−3	−3	−3	−3
5								5	5	5	5
6									6	−5	−5
7											7

[a] See text for details.

[b] The left column is the list of labels used to label the sites of the walk and the top row shows the time steps (or walk site index) at which the label list changes. The body of the table shows the contents of the label list.

Thus whenever a label is looked up in the array of labels with entry $-l$, the algorithm will know that it is invalid, and that the valid label corresponding to the associated site should actually be l (in this case, the algorithm also checks the validity of the label l; if it is also invalid, then this process is repeated until a valid label is found). Going back to Fig. 4, we see that a label conflict occurs at the site immediately following the site labelled 4. Here the label of the preceding site is 4, whereas the nearest neighbour site is labelled 3. Thus the label of the new site becomes 3, and the fourth entry of the array of labels is changed to -3.

When the algorithm finishes traversing the walk, it scans the walk again but this time the correct label for each site is known. The algorithm can then tally up the number of interaction bonds belonging to each cluster in a separate array. In Fig. 4, there are three clusters even though seven labels were used. The first cluster is labelled 1 and contains seven interaction bonds, the second cluster is labelled 5 and contains ten interaction bonds and the last cluster is labelled 7 and contains 2 interaction bonds. The evolution of the label list used in the droplet labelling, as described above, of the example walk in Fig. 4 is given in Table 1.

4. RESULTS

In this section we present the results of the simulations that were performed. We firstly discuss how to interpret the results of the cluster numbers and their preliminary processing. We then examine the specific results for the Manhattan lattice, followed by the results for the simple cubic lattice. All of the simulations presented in this paper were carried out

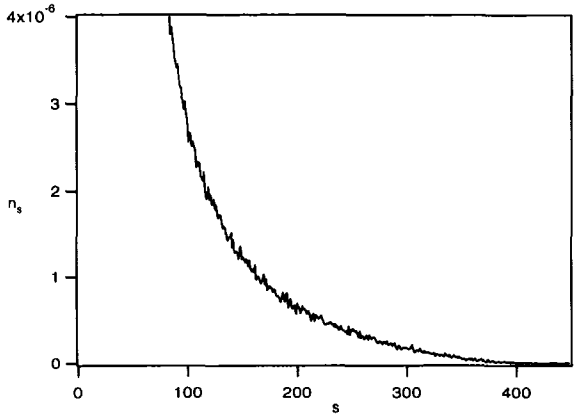

Fig. 5. The same plot as in Fig. 2, but with the largest cluster for each configuration removed from the sample. Note the change in scale on the horizontal axis.

on an 80 node Paragon Intel supercomputer and took roughly 3 months of CPU time to complete. Note, all statistical errors represent 95% confidence intervals, with systematic errors added to the statistical errors.

Figure 2 shows the cluster numbers on the simple cubic lattice for a low temperature ($\omega = 1.405 > \omega_p$), where the typical ISAW configuration is dense. The function has a noticeable "bump" for large s: this is a manifestation of the precursor of the infinite cluster in a finite size system. In ordinary percolation, the bump is usually removed by not including clusters that span the simulation boundaries. In our case, the surface structure of the walk complicates the corresponding operation. We therefore chose the simpler process of not counting the largest cluster in each configuration when compiling the cluster numbers for use in our analysis. We expect this process to be asymptotically equivalent to removing spanning clusters as $N \to \infty$ for $\omega > \omega_p$. This has the effect of removing the bump as well as part of the tail, as can be seen in Fig. 5.

4.1. Simulations on the Manhattan Lattice

We decided to investigate the question of the coincidence of ω_p and ω_θ by performing simulations on the two-dimensional Manhattan lattice. The advantages of simulating on this lattice are twofold. Firstly, the θ point is known exactly: $\omega_\theta = \sqrt{2}$.[8, 9] Secondly, at ω_θ there exists a very fast and efficient algorithm[16, 17, 18, 10] that allows the simulation of very long walks. Thus we can perform simulations at $\omega = \omega_\theta$ to determine the behaviour of

the "typical" cluster size, s_ξ accurately. The significance of this is that if s_ξ is finite, then this implies that $\omega_p > \omega_\theta$.

We used the kinetic growth algorithm[16, 17, 18, 10] to generate 6.3×10^5 independent walks of length $N = 102400$ and 1×10^6 independent walks of length $N = 76800$. We also used an exponential spacing to sample walks of shorter length as suggested by Prellberg and Owczarek.[10] They found that this method virtually eliminated the correlations in the data between different walk lengths.

Before we proceed any further, we note a peculiarity in the cluster numbers for walks on the Manhattan lattice. From our definition, the only way a cluster can contain an odd number of bonds on the Manhattan lattice is if an endpoint of the walk is part of that cluster. This end effect was removed by neglecting all odd numbered clusters in our analysis.

We used (15) to obtain an estimate of s_ξ for the infinite walk. There is a subtlety here, in that (15) is only valid for n_s of *infinite* walks. Thus we had to estimate this function by extrapolating the finite walk n_s values to $N = \infty$. We performed this extrapolation for 40 different s values, assuming a $1/N$ correction term. A fit was then performed to the resulting function using (15) as the fitting function; this is shown in Fig. 6. A χ^2 test revealed that (15) was an excellent fitting function for the data. Our estimate for s_ξ is

$$s_\xi = 2300 \pm 200 \tag{16}$$

thus confirming that $\omega_p > \omega_\theta$.

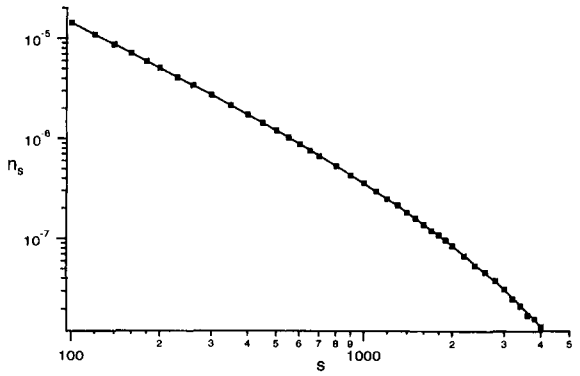

Fig. 6. A fit of (15) to the cluster numbers, n_s for infinite walks on a log-log scale, for the Manhattan lattice. Each data point on this graph was extrapolated from the finite walk $n_s(\omega, N)$ data for $\omega = \omega_\theta$.

The next step was to obtain an estimate of the percolation point, ω_p. We did this by extrapolating the maxima of the various moments of the cluster numbers; this also allowed us to estimate ϕ_p. We used the enhanced R-M algorithm combined with multiple Markov chains[19] to estimate the second, third and fourth moments of the cluster numbers as a function of ω. These simulations were carried out for $800 \leqslant N \leqslant 3200$. In all cases we estimated the autocorrelation times of the relevant observables using the procedure described in Appendix C of ref. 20. This allowed us to estimate how many independent samples of walks were generated by our runs. For $N = 3200$, 1×10^5 independent samples were generated at $\omega = 1.46$ (the exact number of independent configurations generated varied for each temperature since lower temperatures had larger autocorrelation times). We also performed simulations for smaller values of N but we found that they were significantly affected by corrections to scaling and hence omitted.

Figure 7 shows our extrapolation of ω_p from the maxima of the second, third and fourth moments of the cluster numbers. The inset of Fig. 7, shows a typical curve of the third moment of the cluster numbers. The fact that the maxima of the second and third moments approaches ω_p from below whereas the maximum of the fourth moment approaches ω_p from above facilitates a precise estimation of ω_p. Our estimates for ω_p and ϕ_p are

$$\omega_p = 1.461 \pm 0.003 \tag{17}$$

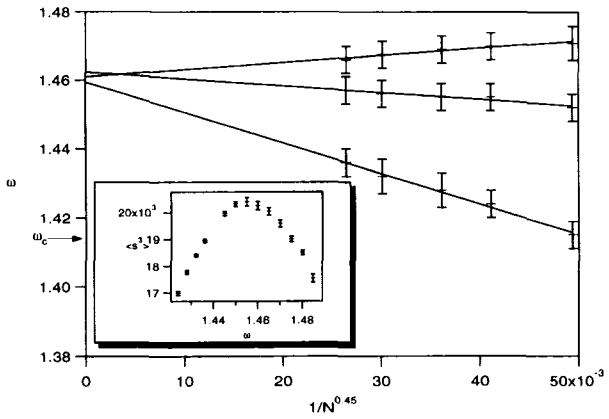

Fig. 7. This plot illustrates our extrapolation procedure used to obtain ω_p for the Manhattan lattice. The curves from the bottom to the top correspond to the maxima of the second, third and fourth moments of the cluster numbers respectively. The inset is the curve of the third moment of the cluster numbers for $N = 2400$.

and

$$\phi_p = 0.45 \pm 0.1 \tag{18}$$

The central estimate of ω_p was fairly insensitive to the value of ϕ_p (e.g., using $\phi_p = 0.55$ and the third and fourth moments gives $\omega_p = 1.462$, whilst using $\phi_p = 0.35$ gives $\omega_p = 1.463$). The error estimates are confidence intervals based on the systematic variation due to ϕ_p and the least squares fits. Note that ω_p is quite distinct from the θ point, $\omega_\theta = \sqrt{2} \approx 1.414$.

We then estimated τ from the divergence of the moments at $\omega = \omega_p$. We performed a number of simulations at $\omega = 1.461$ for $800 \leqslant N \leqslant 6400$. For $N = 6400$, we generated 1×10^5 independent samples. The inset of Fig. 8 is a log-log plot of the second moment of the cluster numbers as a function of N. The slope of this curve for the k-th moment should be $(k + 1 - \tau)$. However there is significant curvature in the data. Thus we calculated local slopes for a range of different N values of the original plot. These local estimates of τ, which we denote τ_{eff} were then extrapolated as shown in Fig. 8. We used our estimate of ϕ_p as the correction-to-scaling exponent in the extrapolation. We also tried a number of other similar techniques; the variation in the estimates of τ was a rough indication of the systematic error. Our estimate for τ based on the above analysis is

$$\tau = 2.25 \pm 0.15 \tag{19}$$

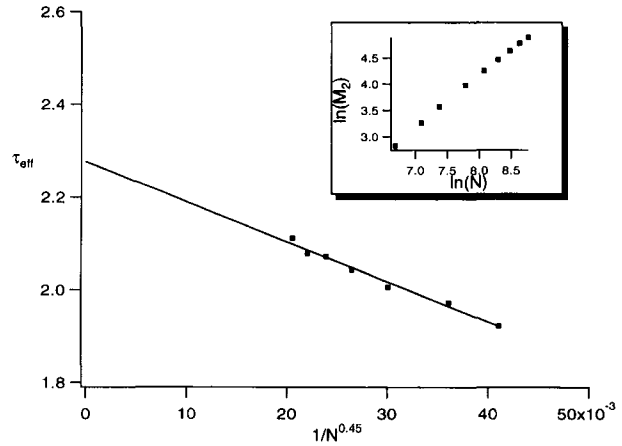

Fig. 8. A plot of the τ_{eff} for the Manhattan lattice. The inset shows a plot of the log of the second moment of the cluster numbers against $\log(N)$ from which the values of τ_{eff} were calculated.

The large uncertainty is due to the large systematic error in the data rather than the statistical error of our simulations.

Finally, we checked the assumption made in Section 2.2 that led to $\phi_p = \sigma$. We did this by assuming that the moments at ω_p diverged as

$$M_k(\omega_p, N) \sim N^{(k+1-\tau)\phi_p/\sigma} \quad \text{as} \quad N \to \infty \tag{20}$$

which can be deduced by using a weaker assumption than that which lead to (11). We then eliminated the ϕ_p/σ factor from the exponent of (20) by taking the ratio of the slopes of the log-log plots of two different moments. This allowed us to make an estimate of τ unbiased by the stronger scaling assumption. We used this value of τ to obtain an independent estimate of ϕ_p/σ. Our estimate for ϕ_p/σ is 0.995 ± 0.01 which is in clear agreement with ϕ_p and σ being equal.

4.2. Simulations on the Simple Cubic Lattice

We performed a large number of simulations on the simple cubic lattice. Our first objective was to estimate the percolation point, ω_p, together with the crossover exponent, ϕ_p. As in the Manhattan analysis we extrapolated the locations of the maxima of the various moments of the cluster numbers (with the largest cluster taken out). We again used the enhanced R-M algorithm combined with multiple Markov chains to estimate the second, third and fourth moments of the cluster numbers as a function of ω. These simulations were carried out for $800 \leqslant N \leqslant 3200$ since smaller values of N were significantly affected by corrections to scaling. For $N = 3200$ we generated 1×10^5 independent samples at $\omega = 1.35$ (the exact number of samples generated depended on the temperature since lower temperatures had larger autocorrelation times).

We found that the maxima of all the moment curves were shifting from right to left, towards both the percolation and θ points. Our estimate for ω_p is

$$\omega_p = 1.325 \pm 0.012 \tag{21}$$

This is slightly above the θ point, ω_θ. (Current estimates of ω_θ are 1.308 ± 0.001[21] and 1.318 ± 0.008.[22] The percolation crossover exponent was also estimated from the above data:

$$\phi_p = 0.55 \pm 0.15 \tag{22}$$

For this estimate of ϕ_p, the locations of the maxima of the moments extrapolated to roughly the same value of ω_p. The central estimate of (22) produced the least scatter for ω_p.

The exponent τ was then estimated from the divergence of the moments at $\omega = \omega_p$ by using (13). Thus we performed a number of simulations at $\omega = 1.325$ for $800 \leqslant N \leqslant 5600$. We generated 1×10^5 independent samples for $N = 5600$. We then performed a similar analysis to that on the Manhattan lattice which resulted in the estimate

$$\tau = 2.3 \pm 0.1 \tag{23}$$

where the error bar is a combination of the statistical and systematic errors.

5. CONCLUSIONS

We have given evidence that there exists a Polymer-Interaction Percolation transition in the ISAW model in two and three dimensions. Evidence suggests that this transition takes place at a temperature lower than the θ point. We have estimated the values of the exponents τ and σ on the Manhattan and simple cubic lattices, as well as the position of the PIP transitions.

ACKNOWLEDGMENTS

The authors take pleasure in thanking A. J. Guttmann for carefully reading the manuscript. Financial support from the Australian Research Council is gratefully acknowledged by the authors.

REFERENCES

1. P. Flory, *Principles of Polymer Chemistry* (Cornell University Press, Ithaca, 1953).
2. P.-G. de Gennes, *J. Physique Lett.* **36**:L55 (1975).
3. J. des Cloizeaux and G. Jannink, *Polymers in Solution* (Clarendon Press, Oxford, 1990).
4. P.-G. de Gennes, *Phys. Lett.* **38A**:339 (1972).
5. P.-G. de Gennes, *J. Physique Lett.* **39**:L299 (1978).
6. A. Coniglio, C. N. Nappi, F. Peruggi, and L. Russo, *J. Phys. A.* **10**:205 (1977).
7. Y. Zhou, C. K. Hall, and M. Karpluts, *Phys. Rev. Lett.* **77**:2822 (1996).
8. R. M. Bradley, *Phys. Rev. A* **39**:3738 (1989).
9. R. M. Bradley, *Phys. Rev. A* **41**:914 (1990).
10. T. Prellberg and A. L. Owczarek, *J. Phys. A.* **27**:1811 (1994).
11. P. P. Nidras and R. Brak, *J. Phys. A.* **30**:1457 (1997).
12. D. Stauffer and A. Aharony, *An Introduction to Percolation Theory* (Taylor and Francis, London, 2nd ed., 1992).
13. R. Brak and A. L. Owczarek, *J. Phys. A.* **28**:4709 (1995).
14. A LaTeX macro to obtain this symbol in displaystyle under 11pt is \,\circ \hspace{-10pt}\sim.

15. J. Hoshen and R. Kopelman, *Phys. Rev. B.* **14**:3438 (1976).
16. I. Majid, N. Jan, A. Coniglio, and H. E. Stanley, *Phys. Rev. Lett.* **52**:1257 (1984).
17. J. Lyklema and K. Kremer, *J. Phys. A.* **17**:L691 (1984).
18. K. Kremer and J. Lyklema, *J. Phys. A.* **18**:1515 (1985).
19. M. C. Tesi, E. J. J. van Rensburg, E. Orlandini, and S. G. Whittington, *J. Stat. Phys.* **82**:155 (1996).
20. N. Madras and A. D. Sokal, *J. Stat. Phys.* **50**:109 (1988).
21. P. Grassberger and R. Hegger, *J. Chem. Phys.* **102**:6881 (1995).
22. M. C. Tesi, E. J. J. van Rensburg, E. Orlandini, and S. G. Whittington, *J. Phys. A.* **29**:2451 (1996).